

PHYSICAL REVIEW B

CONDENSED MATTER

THIRD SERIES, VOLUME 29, NUMBER 10

15 MAY 1984

Bonding of surface states on W(001): All-electron local-density-functional studies

S. Ohnishi

*Department of Physics and Astronomy, Northwestern University, Evanston, Illinois 60201
and NEC Corporation, 1-1 Miyazaki 4-chome, Miyamae-ku, Kawasaki 213, Japan*

A. J. Freeman

*Department of Physics and Astronomy, Northwestern University, Evanston, Illinois 60201
and Lawrence Livermore National Laboratory, Livermore, California 94550*

E. Wimmer

*Department of Physics and Astronomy, Northwestern University, Evanston, Illinois 60201
and Institut für Physikalische Chemie, Universität Wien, A-1090 Vienna, Austria*

(Received 28 November 1983)

Results of self-consistent all-electron full-potential linearized-augmented-plane-wave method local-density-functional calculations are presented for W(001) films consisting of 1, 3, 5, 7, 9, and 8 layers. The theoretical value of the work function for films with five and more layers is found to be within 0.05 eV of the experimental value of 4.63 eV. It is demonstrated that a film of seven layers is sufficiently thick to describe surface states and surface resonance states. An analysis of the dispersion and the change of bonding for the surface (resonance) states of Σ symmetry suggests that the discrepancies between experimental and theoretical surface energy band structures concerning surface states and surface-resonance states near the \bar{M} symmetry point are due to displacements of the surface atoms in the high-temperature phase of the W(001) system.

I. INTRODUCTION

Despite the extensive studies in the past two decades of the W(001) surface, we are still far from a complete understanding of the geometrical and electronic structure of this system. Initially, W was chosen as the prime testing ground for new surface-sensitive experimental techniques because its high thermal stability allows the easy preparation of clean surfaces. Indeed, it was on the W(001) surface that the first metallic surface state was observed by photoemission experiments.^{1,2} Prior to this discovery, this spectroscopic feature had given rise to the observation of an "anomalous" peak in field-emission energy distribution (FEED) curves.³ Early low-energy electron-diffraction (LEED) studies on clean and hydrogen-covered W(001) surfaces led to the observation⁴ that upon cooling from high temperatures the W(001) surface reconstructs from a (1×1) into a $c(2 \times 2)$ structure. Further experimental investigations⁵⁻⁷ established that this reconstruction is a property of the clean surface and is not due to residual hydrogen. As a model to account for this, Felner *et al.*⁵ proposed a vertical displacement of the W atoms at the surface, but Debe and King⁶ found

evidence from LEED, work-function, and Auger-electron-spectroscopy (AES) measurements for a parallel shift of the surface atoms. According to their model,⁶⁻⁸ below 400 K the surface W atoms are displaced alternately by about 0.15–0.30 Å along the $\langle 110 \rangle$ directions, thus forming zigzag chains with a $(\sqrt{2} \times \sqrt{2})R 45^\circ$ unit cell and $p2mg$ two-dimensional space-group symmetry.⁶ An alternative structure involving a parallel shift has been discussed by King and Thomas,⁹ who propose a pairing of surface atoms along the $\langle 110 \rangle$ or $\langle 010 \rangle$ directions.

In addition to the reconstruction of the W(001) surface, analysis of LEED intensities provided evidence for a contraction of the topmost layer in the high-temperature phase by $(6 \pm 6)\%$,¹⁰ $(11 \pm 2)\%$,¹¹ $(4.4 \pm 3)\%$,¹² and $(6.7 \pm 2)\%$.¹³ The variation in these data has given rise to a critical assessment of the LEED analysis.¹⁴ The use of a spin-polarized LEED technique¹⁵ resulted in a value of $(7 \pm 1.5)\%$ for the contraction and backscattering-channeling experiments¹⁶ using mega-electron-volt He^+ ions led to the conclusion that the value for the contraction does not exceed 6%.

This seemingly well-established picture of the reconstruction and relaxation of the W(001) surface has been

questioned in light of recent field-ion microscopy (FIM) studies^{17–19} on this surface. Tsong and Sweeney¹⁷ observed a (1×1) structure even at 21 K, and therefore concluded that the parallel shifts of the surface atoms are less than 0.15 Å. They also raised the possibility of a multilayer reconstruction. Melmed *et al.*¹⁸ found support for the vertical-shift model from their FIM studies on the W(001) surface, but state that “no phase transition may be needed to account for the structural features of W(001).” Recently Tung and Graham¹⁹ observed, with the use of FIM, a reconstructed W(001) surface in the temperature range 15–580 K with surface atoms of alternating height. However, it cannot be completely ruled out¹⁸ that the persistence of the reconstruction (without a parallel shift) at higher temperature could be due to the strong electric field applied in the FIM technique. On the other hand, Stensgaard *et al.*²⁰ claimed, on the basis of ion-scattering experiments, that neither of the two models for the $c(2 \times 2)$ structure is valid; instead, they consider the phase transition as a disorder-order process of the type also discussed by Debe and King.⁶ Further experimental evidence for the vertical displacement has been concluded from surface-weighted effective potentials obtained from low-energy electron-scattering experiments.²¹ It is therefore not surprising that the phase diagram of the W(001) surface cannot be considered to have been completely clarified at this time.

One of the most important techniques for obtaining information about the electronic structure on surfaces is angle-resolved photoemission spectroscopy (ARPES). As mentioned above, the first metallic surface state was observed by this technique^{1,2} on the W(001) surface. The most characteristic spectroscopic features of the W(001) surface as reported by Weng *et al.*²² can be explained without invoking *d*-band—edge effects. Three experimental surface-resonance (SR) bands are now established. (1) A high-lying SR exists 0.3 eV below the Fermi energy, with its highest intensity at the center of the Brillouin zone, and with rapidly decreasing intensity away from normal emission. The symmetry of this state at $\bar{\Gamma}$ is that of *s* and d_{z^2} orbitals. (2) There is a second high-lying SR about 0.8 eV below the first SR. The intensity of this second SR vanishes for normal emission and reaches its maximum intensity at a $|k|$ value of about 0.2–0.3 Å⁻¹ (the edge of the first Brillouin zone in the $\langle 110 \rangle$ direction is at 1.406 Å⁻¹). This state has mainly odd parity with respect to mirror reflection on the (110) plane and contains a small component of even parity. (3) There is a SR band similar to that described in (1) 4.2 eV below the Fermi energy. Remarkably, the experimental dispersion of each of these three SR bands is observed to be less than 0.3 eV.

Further investigations by Campuzano *et al.*^{23,24} using ARPES on the high-temperature (1×1) and the low-temperature $(\sqrt{2} \times \sqrt{2})R 45^\circ$ structures of the W(001) surface showed that states at the Fermi energy disappear in the phase transition. These authors conclude that more than one state is involved in the phase transition, and also that surface-state gapping seems unlikely to play any role in this reconstruction, although they observed²⁴ the opening of a band gap in the surface states near the Fermi en-

ergy at the phase transition. In this context, the midpoint on the $\bar{\Sigma}$ -symmetry line plays a crucial role, because this midpoint becomes the edge of the smaller Brillouin zone after reconstruction. Questions about the role of surface states in the reconstruction have been raised by Holmes and Gustafsson,²⁵ who investigated the dispersion and symmetry of the surface band structure of W(001) by means of high-resolution ARPES experiments, concluding that “surface states play a much smaller role for an understanding of the low-temperature phase of W(001) than proposed.”

This rather inconsistent picture of the W(001) surface obtained by different experimental techniques represents an exciting challenge for theoretical/computational studies. After early theoretical studies^{26–31} using tight-binding fits to existing bulk band structures and non-self-consistent approaches such as a linear combination of muffin-tin orbitals (LCMTO) method,³² the first self-consistent all-electron band-structure calculation for the W(001) surface was performed by Posternak *et al.*,³³ using their linearized—augmented-plane-wave (LAPW) method for thin films.³⁴ These calculations, which modeled the W(001) surface as a single slab consisting of seven atomic layers, provided, for the first time, a complete description of all three experimentally observed resonance bands. In particular, Posternak *et al.*³³ unambiguously identified a true surface state (SS) at ~ 0.3 eV below the Fermi energy—in agreement with the experimentally observed^{1–3} surface-sensitive feature. These authors found that self-consistency was particularly crucial for correctly describing the energy position of the SS at $\bar{\Gamma}$ just below E_F . In addition, it should be noted that the theoretical value for the work function $[(4.5 \pm 0.2) \text{ eV}]$ is in remarkable agreement with experiment (4.63 eV).³⁵

However, a detailed comparison between the theoretical results³³ for the energies and dispersions of the SS and SR bands and recent experimental results^{23–25} show the following severe discrepancies. (1) The high-resolution ARPES experiments of Holmes and Gustafsson²⁵ reveal that along the $\bar{\Sigma}$ -symmetry line the highest SR band, which starts at 0.3 eV below E_F , has a slight upward dispersion away from $\bar{\Gamma}$ and intersects the Fermi level at $k_{||} = 0.6 \text{ \AA}^{-1}$, whereas the theoretical results of Posternak *et al.*³³ suggest an intersection at $k_{||} = 0.1 \text{ \AA}^{-1}$. (2) Holmes and Gustafsson²⁵ report a doublet (even- and odd-component) SS intersecting the Fermi level at 1.2 Å⁻¹, whereas the theoretical result³³ yields an intersection at 0.7 Å⁻¹, i.e., at about the midpoint of the $\bar{\Gamma}\bar{M}$ -symmetry line. (3) Theoretically,³³ the low-lying SS is found about 0.6 eV lower than the experimental²⁵ result. The theoretical and experimental dispersions are in very good agreement for this state.

It is well known that local-density-functional (LDF) eigenvalues are not directly related to excitation energies, and that, in general, the difference between theoretical and experimental bands are due to self-interaction corrections, relaxation, and final-state effects which are known to become more important away from the Fermi energy.³⁶ Since the corrections to the LDF eigenvalues are usually small near E_F , the discrepancies concerning the SS near E_F could be due to assumptions not inherent in the LDF

approach. In fact, this difference between the theoretical surface band structure (which was obtained by assuming a certain geometrical model) and experiment may be an important aspect with which to assess the actual geometrical structure of the W(001) surface.

The calculations by Posternak *et al.*³³ were performed for an idealized W(001) surface by assuming the bulk nearest-neighbor distances to hold for the surface atoms as well. Clearly, this structural model is the natural starting point of any theoretical investigation of the W(001) surface. As a next step, Posternak *et al.*³⁷ investigated the changes in the electronic structure of the W(001) surface states induced by a 6% contraction of the distance between the two topmost layers. The results of this calculation show that such a contraction has a surprisingly small effect on the energies and dispersions of the SS's and SR states. Thus, it can be concluded that a mere contraction is not sufficient to explain the differences between experimental²⁵ and theoretical surface band structures.

However, there remain the following approximations in the calculations of Posternak *et al.*^{33,37} which need to be further elucidated. (1) Posternak *et al.*^{33,37} employed a version of the LAPW method in which the potential was general, except inside the muffin-tin spheres where it was assumed to be spherically symmetric. (2) The W(001) surface was represented by a single slab consisting of seven atomic layers, and thus there are still residual interactions between the two surfaces of the slab which could cloud the results. (3) The valence electrons have been treated by a semirelativistic approach,³⁸ i.e., by neglecting the spin-orbit interaction, but retaining all other relativistic kinematic effects. (4) Finally, one must keep in mind that these calculations are based on the local approximation to density-functional theory (DFT). However, before faulting the LDF, one must assess or eliminate all other approximations not inherent in local DFT. Whereas approximation (3) is believed to be justifiable for describing the SS's and SR states of the W(001) surface,³⁹ and whereas approximation (1), as will be demonstrated below, has no great impact in the present case, the finite-slab approach could be serious, particularly for the W(001) surface because of its richness of SS's and SR states, some of which are decaying rather slowly into the bulklike interior. Thus far, finite-thickness effects have not been studied systematically for the W(001) system using a self-consistent all-electron approach. Thus, one of the aims of the present paper is a detailed analysis of the influence of the film thickness on the W(001) SS's and SR states using the full-potential linearized-augmented-plane-wave (FLAPW) method.⁴⁰ Starting with a W(001) monolayer, self-consistent results for films with 3, 5, 7, 9, and 8 layers will be presented, and the analysis will focus on the energy bands of the SS's and SR states and their dependence on the film thickness. The second purpose of the present work is a detailed analysis of the bonding character of the surface states which disagrees with experiment.

II. METHODOLOGY AND APPROACH

The geometrical structures of the films investigated in the present work are shown in Fig. 1. All systems possess inversion symmetry and have a mirror plane in the center

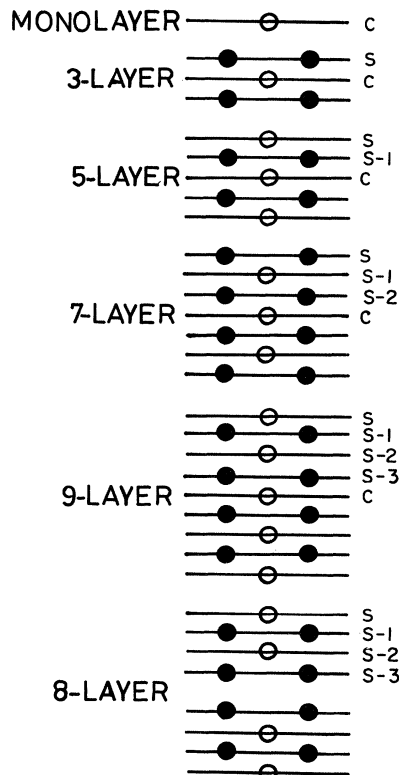


FIG. 1. Geometrical structures of W(001) films investigated in the present work. The positions of the atoms indicated by open and solid circles differ by $(\frac{1}{2}a, \frac{1}{2}a, \frac{1}{2}a)$ where a is the bulk lattice constant of 5.973 a.u.

of the film (z -reflection symmetry). All nearest-neighbor distances, including the surface atoms, are assumed to be bulklike, corresponding to the bulk lattice constant of $a=5.973$ a.u. The electronic structures are calculated on the basis of local DFT (Refs. 41 and 42) using the Wigner exchange-correlation potential.⁴³

Self-consistent solutions of the Kohn-Sham equations are obtained by the FLAPW method for a general (full) potential, and the corresponding terms in the Hamiltonian matrix are treated rigorously in all regions of space, and, in particular, inside the muffin-tin spheres as well. The core states, which are recalculated in each iteration, are treated fully relativistically, and the valence states (originating from the atomic $6s$ and $5d$ orbitals) are calculated semirelativistically.³⁸

As in the previous calculation by Posternak *et al.*,^{33,37} the muffin-tin radii are assumed to be touching along the $\langle 111 \rangle$ directions, and the vacuum boundaries at $z=\pm D/2$ touch the outermost muffin-tin spheres. For the interstitial region the wave functions, charge densities, and potentials are expanded in a Fourier series where the z -dependent part has a periodicity equal to D' where $D' \approx \frac{6}{5}D$. It should be noted, however, that within a full-potential approach such as the FLAPW method the partition of real space is chosen purely as a matter of mathematical convenience and has no effect on the results. For the 1-, 3-, 5-, 7-, and 9-layer films, about 70, 100, 160, 220, and 280 LAPW basis functions are used for

each symmetry type. Inside the muffin-tin spheres, basis functions with angular momentum components up to $l=8$ are included, and the charge density and the potential are expanded in lattice harmonics with $l \leq 8$. The integrals over the irreducible $\frac{1}{8}$ th wedge of the first Brillouin zone are based on a grid of 25 \vec{k} points and are evaluated using a linear triangular interpolation scheme.⁴⁴ Self-consistency is assumed when the input and output densities differ in the average by less than 5×10^{-4} electron/a.u.³

Finally, results of a calculation on a slab of eight layers are reported. This case is equivalent to a nine-layer slab except that the central layer has been removed. This model calculation provides further insight into finite-thickness effects as will be discussed below.

III. RESULTS AND DISCUSSION

A. Charge density and work function

The electronic charge density and the work function as obtained from LDF theory have a direct physical interpretation, and therefore these quantities will be discussed first. In Table I the valence charges inside the touching muffin-tin spheres are listed in the third column. As expected, the charge inside the muffin-tin spheres is found to scale with the number of nearest neighbors. Almost half of the six valence electrons are outside the muffin-tin sphere in the case of the monolayer. For all multilayer

TABLE I. Valence charges inside touching muffin-tin (MT) spheres and work functions of W(001) thin films.

W(001)		Charge in MT sphere	Work function (eV)
Monolayer	C	3.677	5.47
3 layer	S	4.157	4.82
	C	4.480	
5 layer	S	4.141	4.62
	S-1	4.514	
	C	4.525	
7 layer	S	4.151	4.64
	S-1	4.504	
	S-2	4.525	
	C	4.535	
9 layer	S	4.145	4.58
	S-1	4.505	
	S-2	4.521	
	S-3	4.530	
	C	4.511	
8 layer	S	4.161	4.66
	S-1	4.508	
	S-2	4.522	
	S-3	4.127	
Experiment ^a			4.63

^aReference 35.

systems listed in Table I the charges for the surface atoms are about 0.35 electrons less than that of the atoms in the interior of the film. In all cases the subsurface atoms ($S-1$) have almost the same charge as the atoms which are situated deeper inside the film. This result is in agreement with the observation for transition metals that local quantities such as charge densities or magnetic moments are different from the bulk values only for one atomic layer at the surface.^{45,46} It is interesting to note that already for three layers the charges for the surface atoms are close to the value which is found for the thicker films. In the case of the eight-layer film the charges for the atoms at the "inner surface" ($S-3$) are smaller than that for the surface atoms in the three-layer case. This fact is due to the inherent symmetry of the wave functions which reflect the symmetry of the films.

The theoretical work functions for films with more than three layers are found to be in excellent agreement with experiment. The results suggest, for the present case, a theoretical prediction of (4.60 ± 0.05) eV for the work function.⁴⁷ According to a general trend,⁴⁸ the value of the work function of a monolayer is greater (i.e., closer to the atomic ionization potential) than that of the surface.

B. Surface states and surface-resonance states

Figure 2 displays the experimentally determined^{24,25} W(001) surface states and SR states. The theoretical results obtained in the present work are shown in Figs. 3-8. In each of Figs. 3-8, states with even (odd) parity with respect to mirror reflection on the (110) and (100) planes are shown in the lower (upper) panels. States with even (+) and odd (-) parity with respect to mirror reflection in the central plane of the film are represented by dashed and dotted lines, respectively. In the cases with five or more layers, SS's and SR states are marked by thick solid lines. In these plots, the criterion to characterize SS's or SR states is a localization of more than 70% in the surface and subsurface layers.

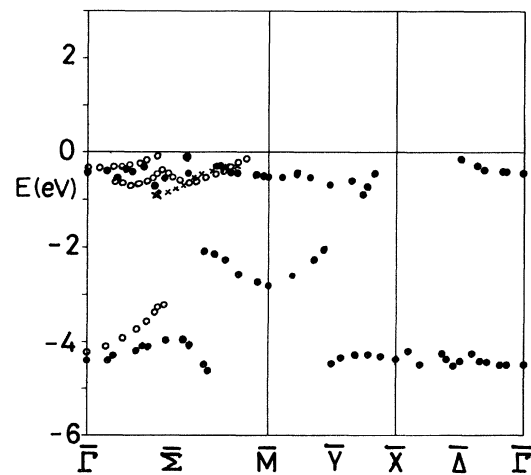


FIG. 2. SS's and SR states as determined from ARPES experiments after Campuzano *et al.* (Ref. 24) (solid circles) and Holmes and Gustaffson (Ref. 25) (open circles, even states; crosses, odd states).

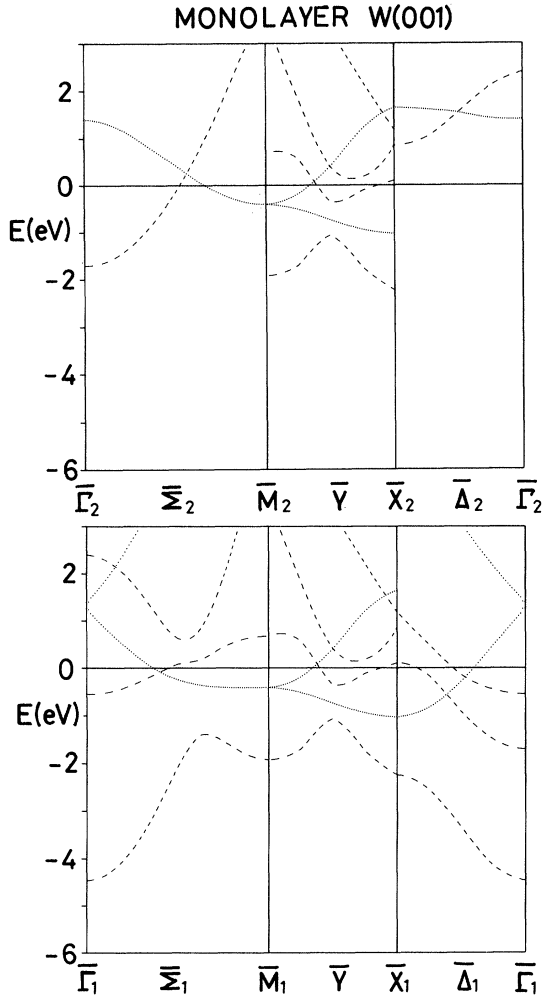


FIG. 3. Theoretical energy-band structure of a W(001) monolayer. Dashed (dotted) lines indicate states which are even (odd) with respect to a mirror reflection on the plane of the atoms. The symmetry indices 1 and 2 refer to mirror reflections on the (110) and (100) planes perpendicular to the film.

The most significant result for the monolayer is a band along $\bar{\Sigma}$ starting at \bar{M} about 0.4 eV below the Fermi energy with an even (1) and odd (2) component. In particular, the even component has almost no dispersion between $\frac{2}{3}\bar{\Gamma}\bar{M}$ and \bar{M} . The states of these bands have $d_{xz,yz}$ character, and hence show odd parity (—) with respect to z reflection. The bonding formed by these states⁴⁹ contributes markedly to the cohesive energy of the monolayer. It is most significant that none of the W(001) multilayer systems (cf. Figs. 4–8) exhibit states at the Fermi energy along the $\bar{\Sigma}$ -symmetry line near the Brillouin-zone boundary, which would explain the surface-sensitive features observed in photoemission experiments (cf. Fig. 2). It is only the isolated monolayer which shows states in the above-mentioned energy and \bar{k} -space range. Comparing the cases with 3, 5, 7, 9, and 8 layers it can be convincingly concluded (cf. Figs. 4–8) that this absence of states along $\bar{\Sigma}$ near \bar{M} is not due to finite-thickness effects. In

fact, even a film of only three layers (Fig. 4) shows essentially those structures which evolve into the SS's and SR states so clearly evident in the thicker films (cf. Figs. 5–8).

In all of the W(001) multilayer films investigated a very characteristic SS band exists along the symmetry line $\bar{\Sigma}$ starting near $\bar{\Gamma}$ at about 0.5 eV below the Fermi energy. With increasing $k_{||}$, this state has a moderate upward dispersion intersecting the Fermi energy at about $\frac{3}{5}\bar{\Gamma}\bar{M}$ and then rising steeply towards \bar{M} , where its energy is about 2 eV above E_F . Between $\frac{1}{5}\bar{\Gamma}\bar{M}$ and $\frac{4}{5}\bar{\Gamma}\bar{M}$ this state is very much localized in the surface region. Therefore the symmetric (+) and antisymmetric (—) partners are practically degenerate even for a film of only five layers, and we will focus only on the symmetric (+) states in the following.

Figures 9 and 10 show the single-state charge densities of the states which are indicated in the band-structure

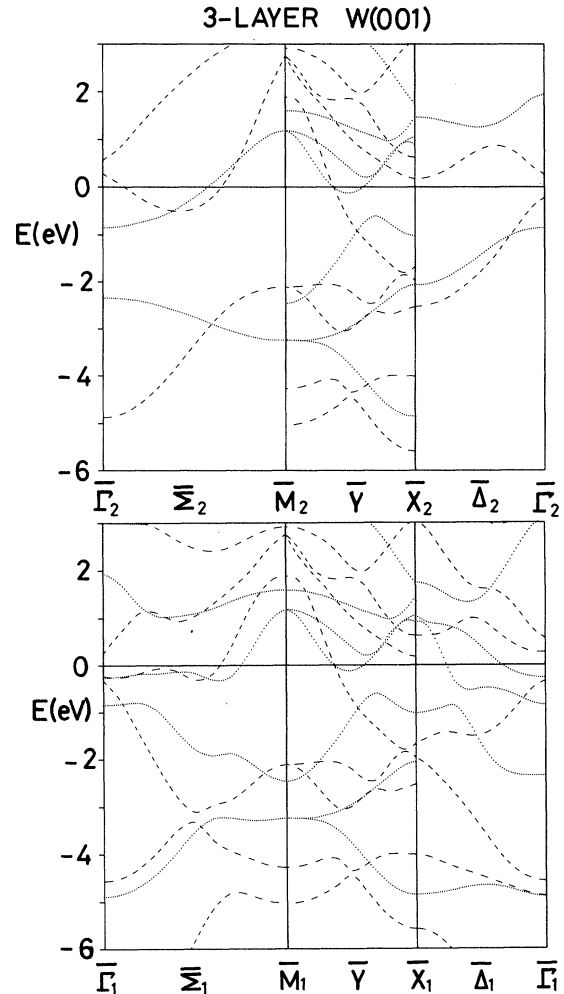


FIG. 4. Energy-band structure of a three-layer W(001) film. Dashed (dotted) lines indicate states which are even (odd) with respect to a mirror reflection on the plane of the central atoms. The labels 1 and 2 have the same meaning as in Fig. 3.

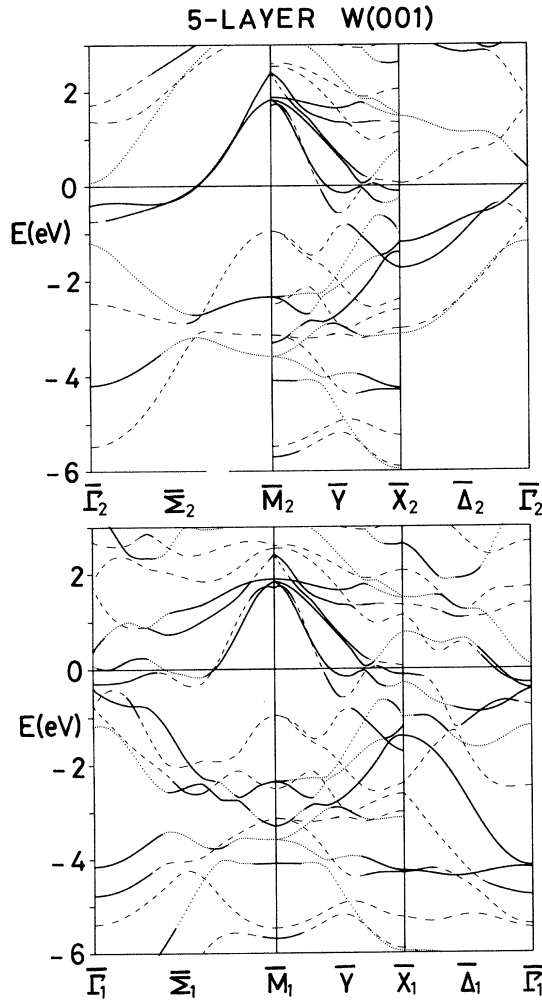


FIG. 5. Energy-band structure of a five-layer W(001) film. Solid lines indicate SS's and SR states with more than 90% charge within the surface and subsurface layers. Otherwise, the same conventions are used as in Fig. 4.

plot (Fig. 6) by $A+$ and $B+$. Comparing the plots of Figs. 9 and 10 for $\vec{k}=(0.3,0.3)$ and $\vec{k}_{||}=(0.8,0.8)$ gives some insight into the change of bonding character: These states have both $d_{x^2-y^2}$ and $d_{xz,yz}$ components. At small values of $k_{||}$ the $d_{x^2-y^2}$ component leads to strong bonding between atoms within the surface layer [cf. Fig. 9(a)]. In addition, the $d_{xz,yz}$ components give rise to pronounced bonding between atoms in the surface and the subsurface layers [cf. the overlap between the lower lobes of the surface atom and the upper lobes of the subsurface atoms as shown in Fig. 10(a)]. At larger values of $k_{||}$, the $d_{x^2-y^2}$ component is weakened [compare Figs. 9(a) and (b)]. The bonding due to $d_{xz,yz}$ components between surface and subsurface atoms changes its character: the upper lobes of the surface atoms now overlap with the upper lobes of the subsurface atoms [cf. Fig. 10(b)]. This change of bonding also manifests itself in the charge-density plot parallel to the surface [Fig. 9(b)] by the appearance of

structures along the diagonals. This change in bonding causes the sharp upward dispersion for $k_{||} > \frac{3}{5}\bar{\Gamma}\bar{M}$.

The highly localized SS with $\bar{\Sigma}_2$ symmetry has a SS counterpart with $\bar{\Sigma}_1$ symmetry near E_F which is much less localized in the surface region. This can be seen by the rather large splitting of the even (+) and odd (-) partners even for thick films (cf. $E+$ and $E-$ in Fig. 6, and the corresponding charge-density plots shown in Fig. 11). Figure 11 illustrates the d_{z^2} -like symmetry and the rather extended nature of this state. For $k_{||} > \frac{3}{5}\bar{\Gamma}\bar{M}$ this state shows a steep upward dispersion similar to the SS discussed above. This upward dispersion is not present for an unsupported W(001) monolayer, where we find states of $d_{xz,yz}$ symmetry about 0.5 eV below E_F near the Brillouin-zone boundary at \bar{M} . Owing to the absence of bonding interactions between the surface and subsurface atoms in the monolayer, the $d_{xz,yz}$ -derived states appear at

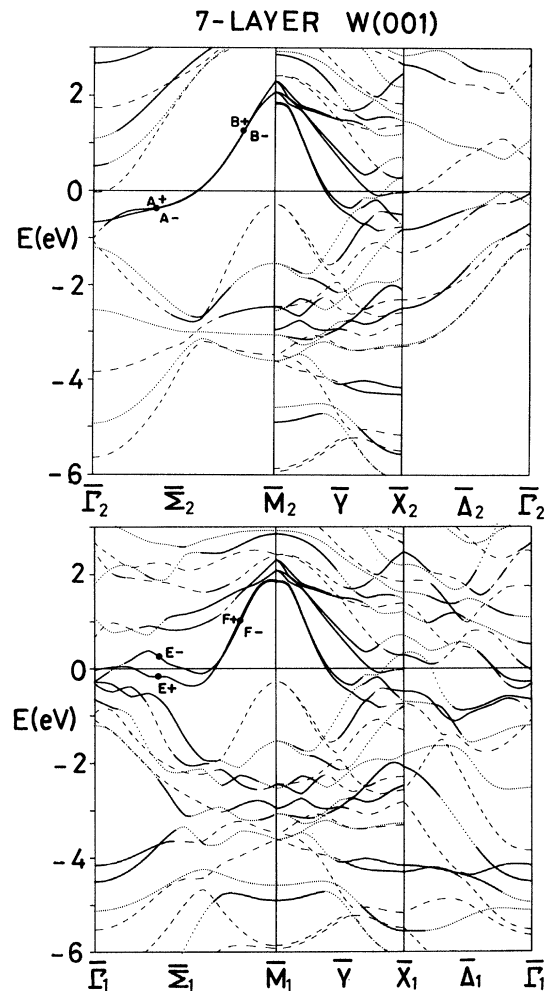


FIG. 6. Energy-band structure of a seven-layer W(001) film. Solid lines indicate SS's and SR states with more than 70% localization within the surface and subsurface atoms. Otherwise, the same conventions are used as in Fig. 4.

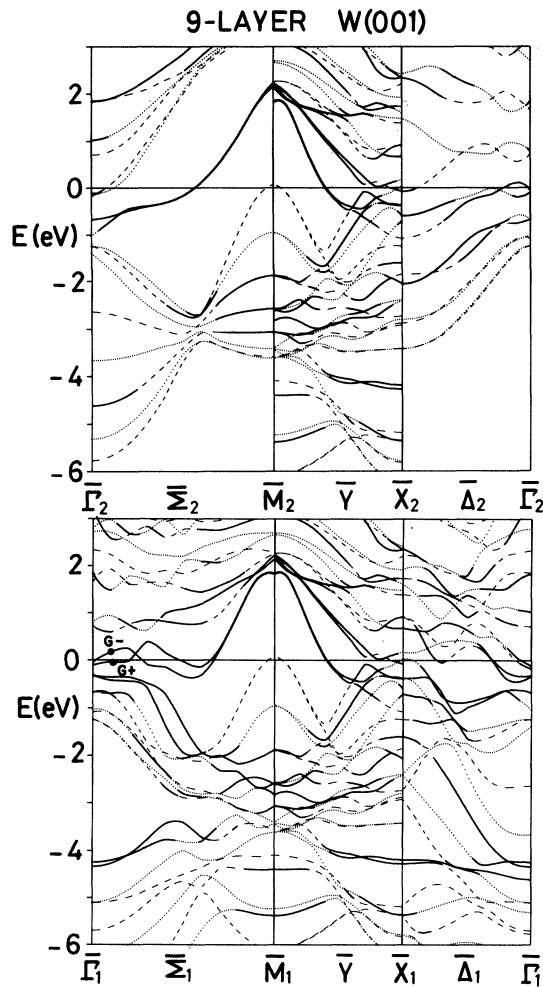


FIG. 7. Energy-band structure of a nine-layer W(001) film. Solid lines indicate SS's and SR states with more than 55% localization within the surface and subsurface atoms. Otherwise, the same conventions are used as in Fig. 4.

small $k_{||}$ values about 1 eV above E_F (cf. dotted lines in Fig. 3), whereas in the multilayer systems these states are found below E_F for small $k_{||}$.

Let us briefly summarize the theoretical results at this point. For an unreconstructed W(001) surface we find a doublet of SS's with $\bar{\Sigma}_1$ and $\bar{\Sigma}_2$ symmetries starting near $\bar{\Gamma}$ just below E_F , with an essentially gentle upward dispersion for small $k_{||}$ intersecting E_F at about $\frac{3}{5}\bar{\Gamma}\bar{M}$. For increasing $k_{||}$ these states show a steep upward dispersion, reaching an energy of about 2 eV above E_F at \bar{M} . This characteristic dispersion is not an artifact due to finite film thickness, but rather it appears to be a property of the unreconstructed, bulklike surface. The sharp upward dispersion is mainly caused by interactions between the surface and subsurface layers. Photoemission experiments^{24,25} clearly show SS's near the zone boundary at \bar{M} about 0.5 eV below E_F .

Photoemission experiments reveal, at normal emission ($\bar{\Gamma}$), two very characteristic SS's, namely a low-lying (LL) SS at 4.3 eV below the Fermi energy and a high-lying (HL) SS at 0.3 eV below E_F . Our theoretical results for

the energies of these states are presented in Table II. It is found that for films with seven and nine layers the agreement between the local DFT one-particle energies and the excitation energies observed in photoemission experiments^{24,25} is remarkable. From the splitting between the even (+) and odd (-) partners it can be seen (cf. Figs. 6 and 7, and Table II) that a film with seven atomic layers is sufficiently thick to adequately describe these SS's. The charge-density plots of the LL (Fig. 12) and HL (Fig. 13) SS's at $\bar{\Gamma}$ for a nine-layer film illustrate the d_{z^2} -like character of both states. These plots (Figs. 12 and 13) also reveal that the LL SS is more extended than the HL SS. Therefore, the even (+) and odd (-) partners are much more split for the LL SS than for the HL SS (cf. Table II).

Away from $\bar{\Gamma}$ the LL SS is found to have an upward dispersion (cf. Fig. 7) and fades away at about $\frac{3}{5}\bar{\Gamma}\bar{M}$, in good agreement with experiment (cf. Fig. 2). Between $\frac{3}{5}\bar{\Gamma}\bar{M}$ and \bar{M} there are rather diffuse SS's and SR states between -2 and -3 eV, with an overall downward dispersion towards \bar{M} (Figs. 5-7). Again, this feature is

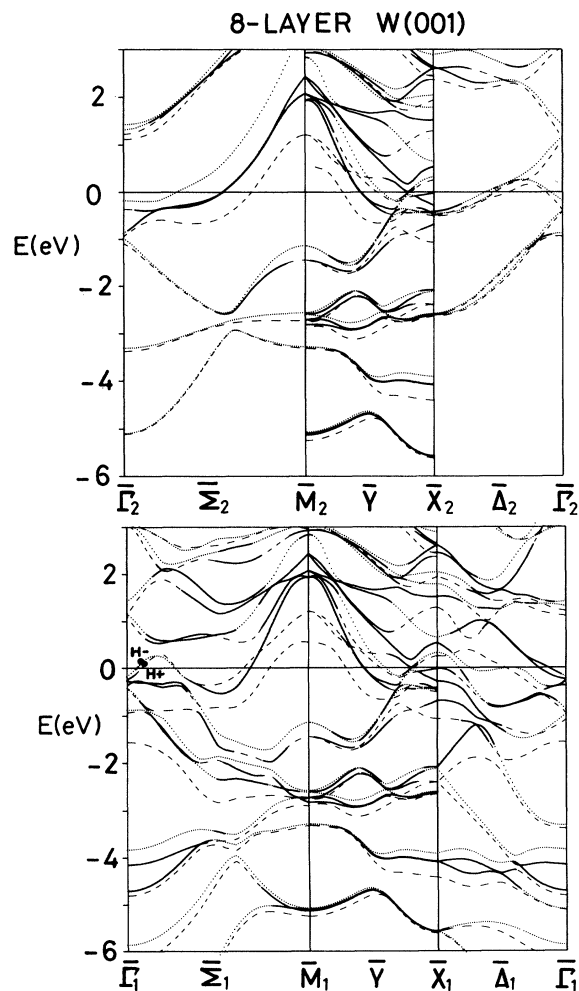


FIG. 8. Energy-band structures of an eight-layer W(001) film. The same conventions are used as in Fig. 7.

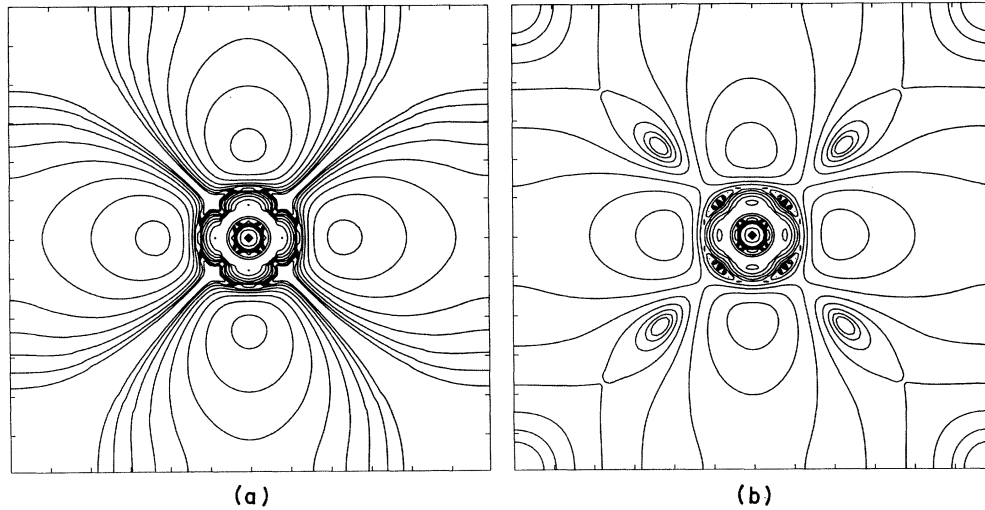


FIG. 9. Charge density of the $\bar{\Sigma}_2(+)$ SR states in a seven-layer W(001) film (labeled $A+$ and $B+$ in Fig. 6) shown for an intersection in the plane of the surface atoms for (a) $\vec{k}=(0.3,0.3)\bar{\Gamma}\bar{M}$ and (b) $\vec{k}=(0.8,0.8)\bar{\Gamma}\bar{M}$. The lowest contour is at a value of 1.0×10^{-3} electron/a.u.³, and subsequent contour lines differ by a factor of 2.

in agreement with structures observed in photoemission experiments.^{24,25}

Along the edge of the first Brillouin zone (symmetry line \bar{Y}), these diffuse SS's and SR states are continued about half the way from \bar{M} to \bar{X} (cf. Figs. 5–7), with an overall upward dispersion away from \bar{M} , also in agreement with experiment (cf. Fig. 2). Along the symmetry line $\bar{\Delta}$ the LL SS at $\bar{\Gamma}$ continues as a SR state with almost no upward dispersion, and from \bar{X} this state extends about half of the way toward \bar{M} (cf. Fig. 2). Theoretically, this feature is found with the same characteristics (cf. Figs. 5–8). In agreement with experiment, the HL SS at $\bar{\Gamma}$ is

found to continue with an upward dispersion from $\bar{\Gamma}$ towards \bar{X} intersecting E_F at about $\frac{1}{3}\bar{\Gamma}\bar{X}$ (cf. Figs. 2 and 5–8).

Significantly, Campuzano *et al.*²⁴ found, from their photoemission experiments, SS's along \bar{Y} about 0.5 eV below E_F which are a continuation of the SS's along the $\bar{\Sigma}$ -symmetry line discussed above. The theoretical studies for the bulklike W(001) surface do not give any SS's or SR states in this region of \vec{k} space or energy.

The results obtained for the model with eight W(001) layers (Fig. 8), where the central layer of the nine-layer film has been removed, provide further evidence that

TABLE II. LDF one-particle energies for the LL and HL W(001) SS's at $\bar{\Gamma}$ compared with photoemission results (Refs. 24 and 25).

Thickness	Symmetry	E (eV)	Average energy (eV)	Localization in layers S and $S-1$ (in %)
LL				
5	+	4.77	4.46	95
	–	4.14		98
7	+	4.16	4.34	79
	–	4.51		95
9	+	4.34	4.29	84
	–	4.24		76
Experimental			4.3	
HL				
5	+	0.76	0.59	89
	–	0.41		99
7	+	0.33	0.31	98
	–	0.28		98
9	+	0.31	0.32	98
	–	0.32		98
Experimental			0.3	

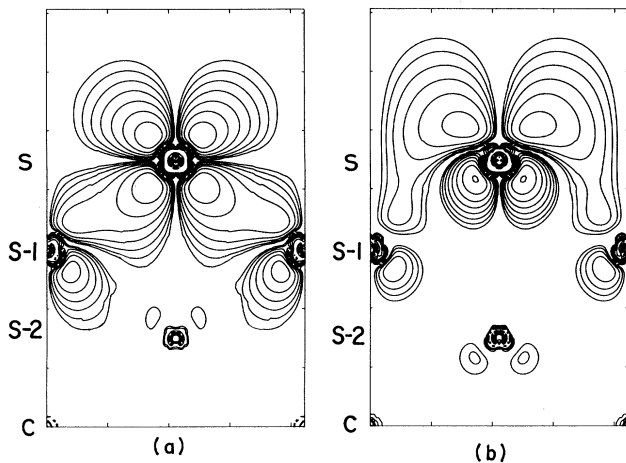


FIG. 10. Charge density of the $\bar{\Sigma}_2(+)$ SR states (same as in Fig. 9) for an intersection in the (110) plane perpendicular to the surface.

W(001) films of seven or nine layers are sufficiently thick to describe true surface phenomena. The band structures for the eight- and nine-layer films exhibit the same features as far as the averaged energies and dispersions of the SS's and SR states are concerned. The absence of a central layer greatly reduces the interaction between SS's and SR states on both sides of the slab. Consequently, pairs of states with even (+) and odd (-) parity with respect to z reflection become almost degenerate (compare Figs. 7 and 8). This effect is particularly obvious for states of $\bar{\Sigma}_1(+)$ and $\bar{\Sigma}_1(-)$ symmetry. This point is illustrated by the single-state charge-density plots (Figs. 14 and 15) for $\bar{\Sigma}_1$ states near $\bar{\Gamma}$ marked by $G+$ and $G-$ (Fig. 7) and $H+$ and $H-$ (Fig. 8), respectively. The extension of these states throughout the entire slab (Figs. 14 and 15) leads to a considerable splitting between the even

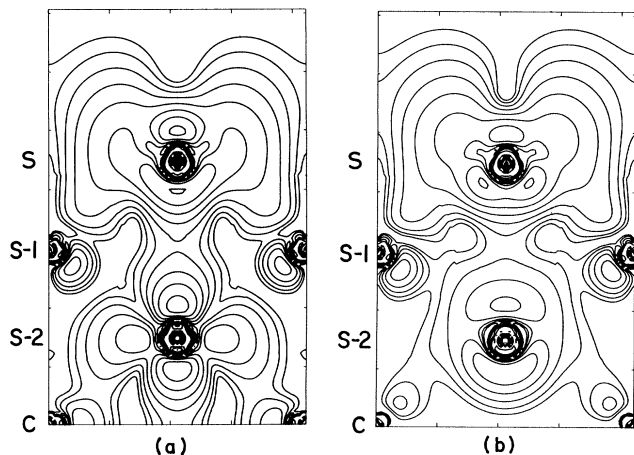


FIG. 11. Charge density of (a) the $\bar{\Sigma}_1(+)$ and (b) the $\bar{\Sigma}_1(-)$ SR states at $\vec{k}=(0.8,0.8)\bar{\Gamma}\bar{M}$ for a seven-layer W(001) film. These states are indicated by $F+$ and $F-$ in Fig. 6. The same contour values and spacings are used as in Fig. 9.

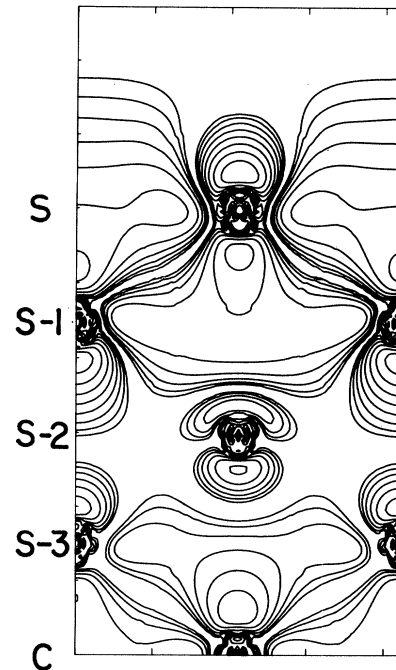


FIG. 12. Charge density of a LL SS $[\bar{\Gamma}_1(+)]$ for a nine-layer W(001) film. Same contour conventions as in Fig. 9.

and odd partners even for a nine-layer film. The results for the eight-layer film clearly reveal the connectivity and anticrossings of s - and d -like surface bands along the symmetry line $\bar{\Sigma}$ (Fig. 8): The HL SS of d_{z^2} character at $\bar{\Gamma}$, 0.3 eV below E_F , is connected to a d -like SR band with

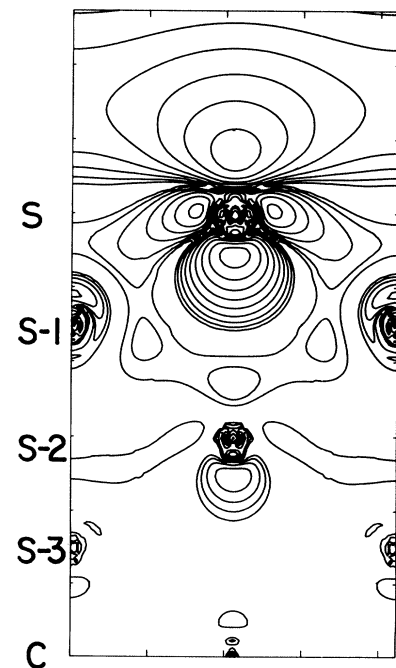


FIG. 13. Charge density of the HL SS $[\bar{\Gamma}_1(+)]$ for a nine-layer W(001) film. Same contour conventions as in Fig. 9.

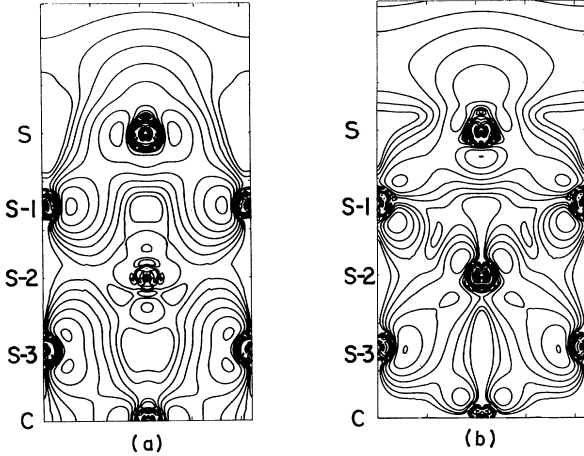


FIG. 14. Charge density of (a) even and (b) odd SR states of Σ_1 symmetry at $\vec{k}=(0.1,0.1)\bar{\Gamma}\bar{M}$ in a nine-layer W(001) film. These states are labeled as $G+$ and $G-$ in Fig. 7. Contour conventions as in Fig. 9.

almost no dispersion between $\bar{\Gamma}$ and $\frac{1}{3}\bar{\Gamma}\bar{M}$, where it reaches an anticrossing. An s -like band (cf. Figs. 8 and 15) starts slightly above the HL SS with a pronounced upward dispersion reaching an anticrossing at about $\frac{1}{5}\bar{\Gamma}\bar{M}$. The other band involved in this anticrossing can be seen to start at $\bar{\Gamma}$ at about 1.2 eV above E_F with a downward dispersion. The dispersion and anticrossings of the corresponding band in the nine-layer film (Fig. 7) are much less evident, and the eight-layer—model calculation (Fig. 8) proves to be very helpful in clarifying this point. As expected, the “inner surface” in the eight-layer model introduces new features in the band structure (cf. Figs. 7 and 8), particularly around \bar{M} about 1 eV above the Fermi energy.

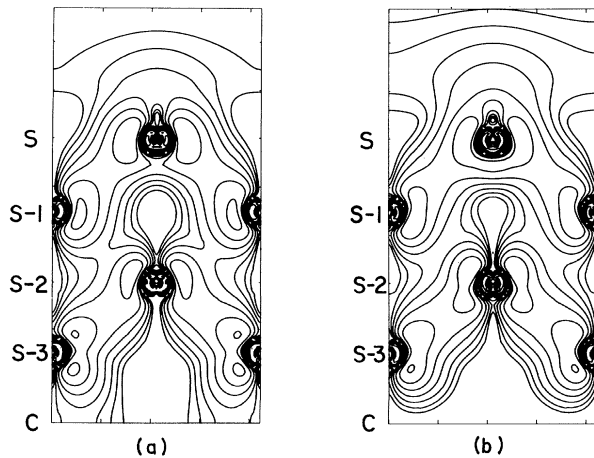


FIG. 15. Charge density of (a) even and (b) odd Σ SR states at $\vec{k}=(0.1,0.1)\bar{\Gamma}\bar{M}$ in an eight-layer W(001) film. These states are labeled as $H+$ and $H-$ in Fig. 9. Contour conventions as in Fig. 9.

IV. SUMMARY AND CONCLUSIONS

We have presented the results of highly accurate self-consistent all-electron local DFT calculations for 1-, 3-, 5-, 7-, and 9-layer W(001) films. An additional model calculation has been performed for an eight-layer film constructed from the nine-layer film by removing the central layer. The all-electron LDF equations have been solved by using the FLAPW method for thin films. In this method a general potential is treated rigorously in all regions of space. The present systematic study reveals that W(001) films with seven layers are sufficiently thick to describe true surface phenomena. All calculations are based on the geometry of a bulklike surface, i.e., the nearest-neighbor distances are assumed to have the bulk values for the surface atoms as well. The work function is found to be within 0.05 eV of the experimental value for films with five and more layers.

Comparison with available ARPES results reveals the following facts: The energy and the dispersion of SS's of predominantly d_{z^2} -like character are excellently reproduced by the present calculation. Thus, for example, we find the LL and HL SS's at $\bar{\Gamma}$ within experimental error. These states project far out into the vacuum, and, due to their character, do not interact strongly with the subsurface layer. In contrast, SS's with important components of $d_{xz,yz}$ character, particularly along the Σ -symmetry line, and which are found experimentally about 0.5 eV below E_F around the symmetry point \bar{M} , have no theoretical counterpart in the present calculations. It has been demonstrated, for $k_{||}$ values near the Brillouin-zone boundary, that these states are shifted about 2 eV above E_F due to a repulsive interaction along the $\langle 111 \rangle$ direction between the surface and subsurface atoms. In the monolayer, where these interactions are absent, we do find these states at \bar{M} some 0.5 eV below E_F .

Considering the fact that (i) the differences between the photoemission results and the theoretical studies are not merely due to relaxation, as has been shown by Posternak *et al.*,³⁷ (ii) they are not due to methodological approximations such as the neglect of nonspherical terms in the potential or finite-thickness effects, as has been shown in the present work, and (iii) the inclusion of spin-orbit splitting does not substantially change the surface band structure,³⁹ we come to the following conclusions. (1) The difference between the photoemission data and the theoretical results is due to different geometrical structures underlying the experiments and the calculations, or, alternatively, (2) the LDF one-particle energies as obtained from the present calculations are fundamentally different from the spectroscopic features observed for the SS's near \bar{M} . It would be very surprising for the present calculations to describe so excellently the energies and dispersions of SS's and SR states throughout most of the first Brillouin zone, and, at the same time, to completely fail to describe the SS's and SR states near the \bar{M} -symmetry point.

We have investigated the electronic origin of the strong upward dispersion of SR states along $\bar{\Gamma}$, which leads to the severe discrepancy between theoretical and experimental results. It has been demonstrated that for these states

the change of bonding between atoms in the surface and subsurface layers upon going from $\bar{\Gamma}$ to \bar{M} is a main cause for their high energy near \bar{M} . Lateral and/or vertical rearrangement of the surface atom along the [110] direction, which would break the symmetry, could prevent this energetically unfavorable change of bonding. Consequently, the one-particle energy of these states would drop below E_F , where they are observed in photoemission experiments. If this rearrangement would occur in a more or less random manner, as suggested by Stensgaard *et al.*,²⁰ with a short-range ordering (if any) below the coherence length of LEED electrons, no conflict would arise between this model and the observation of a (1×1) LEED pattern for the W(001) high-temperature phase. The transition from the (1×1) to the $c(2 \times 2)$ structure would then be a disorder-order transition.²⁰

Very recently, Bullett and Stephenson⁵⁰ obtained evidence from tight-binding calculations that a lateral dis-

placement of the surface atoms strongly influences the Σ_2 SS band, which is exactly the band which is in disagreement with the photoemission data.

In conclusion, it is clear that further experimental and theoretical investigations will be necessary to completely understand the phase diagram of the W(001) surface. In particular, a reassessment of the contraction of the "unreconstructed" W(001) surface will be necessary.

ACKNOWLEDGMENTS

This work was supported by the National Science Foundation (Grant No. DMR82-16543) and the Department of Energy. It is also a pleasure for us to acknowledge the excellent cooperation and the competent service of the Lawrence Livermore Laboratory Computing Center.

- ¹B. J. Waclawski and E. W. Plummer, *Phys. Rev. Lett.* **29**, 783 (1972).
- ²B. Feuerbacher and B. Fitton, *Phys. Rev. Lett.* **29**, 786 (1972).
- ³L. W. Swanson and L. C. Crouser, *Phys. Rev. Lett.* **16**, 389 (1966).
- ⁴Y. Yomehara and L. D. Schmidt, *Surf. Sci.* **25**, 238 (1971).
- ⁵T. E. Felner, R. A. Barker, and P. J. Estrup, *Phys. Rev. Lett.* **38**, 1138 (1977).
- ⁶M. K. Debe and D. A. King, *Phys. Rev. Lett.* **39**, 708 (1977); *J. Phys. C* **10**, L303 (1977); *Surf. Sci.* **81**, 193 (1979).
- ⁷R. A. Barker, P. J. Estrup, F. Jona, and P. M. Marcus, *Solid State Commun.* **25**, 375 (1978).
- ⁸J. Walker, M. K. Debe, and D. A. King, *Surf. Sci.* **104**, 405 (1981).
- ⁹D. A. King and G. Thomas, *Surf. Sci.* **92**, 201 (1980).
- ¹⁰M. A. Van Hove and S. Y. Tong, *Surf. Sci.* **54**, 91 (1976).
- ¹¹B. W. Lee, A. Ignatiev, S. Y. Tong, and M. A. Van Hove, *J. Vac. Sci. Technol.* **14**, 291 (1977).
- ¹²M. K. Debe, D. A. King, and F. Marsh, *Surf. Sci.* **68**, 437 (1977).
- ¹³L. J. Clarke and L. Morales De La Garza, *Surf. Sci.* **9**, 419 (1980).
- ¹⁴M. N. Read and G. Russell, *Surf. Sci.* **88**, 95 (1979).
- ¹⁵R. Feder and J. Kirschner, *Surf. Sci.* **103**, 75 (1981).
- ¹⁶L. C. Feldman, R. L. Kauffmann, P. J. Silverman, R. A. Zuhr, and J. H. Barrett, *Phys. Rev. Lett.* **39**, 38 (1977).
- ¹⁷T. T. Tsong and J. Sweeney, *Solid State Commun.* **30**, 767 (1979).
- ¹⁸A. J. Melmed, R. T. Tung, W. R. Graham, and G. D. W. Smith, *Phys. Rev. Lett.* **43**, 1521 (1979).
- ¹⁹R. T. Tung and W. R. Graham, *Surf. Sci.* **115**, 576 (1982).
- ²⁰I. Stensgaard, L. C. Feldman, and P. J. Silverman, *Phys. Rev. Lett.* **42**, 247 (1979).
- ²¹M. A. Stevens and G. J. Russell, *Solid State Commun.* **34**, 785 (1980).
- ²²Shang-Lin Weng, E. W. Plummer, and T. Gustafsson, *Phys. Rev. B* **18**, 1718 (1978).
- ²³J. C. Campuzano, D. A. King, C. Somerton, and J. E. Inglesfield, *Phys. Rev. Lett.* **45**, 1649 (1980).
- ²⁴J. C. Campuzano, J. E. Inglesfield, D. A. King, and C. Somerton, *J. Phys. C* **14**, 3099 (1981).
- ²⁵M. I. Holmes and T. Gustafsson, *Phys. Rev. Lett.* **47**, 443 (1981).
- ²⁶R. Feder and K. Sturm, *Phys. Rev. B* **12**, 437 (1975).
- ²⁷N. V. Smith and L. F. Mattheiss, *Phys. Rev. Lett.* **37**, 1494 (1976).
- ²⁸M. C. Desjonqueres and F. Cyrot-Lackmann, *J. Phys. F* **6**, 567 (1976).
- ²⁹O. Bisi, C. Calandra, P. Flaviani, and F. Manghi, *Solid State Commun.* **21**, 121 (1977).
- ³⁰B. Lacks and C. F. T. Gonçalves da Silva, *Solid State Commun.* **25**, 401 (1978).
- ³¹W. R. Grise, D. G. Dempsey, L. Kleinman, and K. Mednick, *Phys. Rev. B* **20**, 3045 (1979).
- ³²R. V. Kasowski, *Solid State Commun.* **17**, 179 (1975).
- ³³M. Posternak, H. Krakauer, A. J. Freeman, and D. D. Koelling, *Phys. Rev. B* **21**, 5601 (1980).
- ³⁴H. Krakauer, M. Posternak, and A. J. Freeman, *Phys. Rev. B* **19**, 1706 (1979).
- ³⁵R. L. Billington and T. N. Rhodin, *Phys. Rev. Lett.* **41**, 1602 (1978).
- ³⁶J. P. Perdew and A. Zunger, *Phys. Rev. B* **23**, 5048 (1981).
- ³⁷M. Posternak, H. Krakauer, and A. J. Freeman, *Phys. Rev. B* **25**, 755 (1982).
- ³⁸D. D. Koelling and B. N. Harmon, *J. Phys. C* **10**, 3107 (1977).
- ³⁹L. F. Mattheiss and D. R. Hamann, *Bull. Am. Phys. Soc.* **27**, 210 (1982), and unpublished.
- ⁴⁰E. Wimmer, H. Krakauer, M. Weinert, and A. J. Freeman, *Phys. Rev. B* **24**, 864 (1981), and references therein.
- ⁴¹P. Hohenberg and W. Kohn, *Phys. Rev.* **136**, B864 (1964).
- ⁴²W. Kohn and L. J. Sham, *Phys. Rev.* **140**, A1133 (1965).
- ⁴³D. Pines, *Elementary Excitations in Solids* (Benjamin, New York, 1963), Eq. (3.58).
- ⁴⁴C. S. Wang and A. J. Freeman, *Phys. Rev. B* **21**, 4585 (1980), and references therein.
- ⁴⁵E. Wimmer, A. J. Freeman, and H. Krakauer, *Phys. Rev. B* (to be published).
- ⁴⁶S. Ohnishi, A. J. Freeman, and M. Weinert, *Phys. Rev.* **28**, 6741 (1983).
- ⁴⁷The slightly higher value of 4.77 eV for the work function of a

- five-layer W(001) slab reported earlier by E. Wimmer, A. J. Freeman, M. Weinert, H. Krakauer, J. R. Hiskes, and A. M. Karo [Phys. Rev. Lett. **48**, 1128 (1982)] is presumably due to the coarser \vec{k} -point grid (19 \vec{k} points) and a simple histogram-integration technique used in this earlier work.
- ⁴⁸E. Wimmer, J. Phys. F **13**, 2313 (1983).
- ⁴⁹A similar type of bonding is observed for linear chains of Fe and Ni atoms: A. J. Freeman and M. Weinert, Bull. Am. Phys. Soc. **27**, 180 (1982); M. Weinert and A. J. Freeman, J. Magn. Magn. Mater. **38**, 23 (1983).
- ⁵⁰D. W. Bullett and P. C. Stephenson, Solid State Commun. **45**, 47 (1983).